

Autoadaptive Mesh Refinement

Claude Simon^{■▲}, Serge Mottet[■] and Jean Emmanuel Viallet[■]

■ *Centre National d'Etudes des Télécommunications - 22301 Lannion - France*

▲ *Institut de Recherche en Informatique et Systèmes Aléatoires*

Campus de Beaulieu - 35042 Rennes Cedex - France

Abstract

An autoadaptive mesh refinement method is described. Using a Box Method discretization scheme, we compute a local error arising from the difference between the physical and the discretized problem. This error indicates where the mesh must be refined. The refinement strategy is applied to the simulation of several semiconductor devices, including III-V optoelectronic devices.

The autoadaptive mesh refinement method is closely related to the discretization scheme used. On the other hand, the discretization scheme has to be adapted to the physical equations when simulating the electrical properties of today devices. An overview of the physical model is briefly made, in order to precise the type of mathematical expressions that the discretization scheme has to deal with. Then, the discretization scheme and the proposed autoadaptive method are presented.

1 PHYSICAL MODEL

Steady state electrical conduction in semiconductors is basically described by the three following equations (Poisson equation and the two continuity equations) :

$$(1) \quad \text{div}(\epsilon \cdot \overrightarrow{\text{grad}} \varphi) = q \cdot (n - p - \text{dop}) ; \quad - \frac{1}{q} \cdot \text{div} \overrightarrow{J}_n = - U ; \quad \frac{1}{q} \cdot \text{div} \overrightarrow{J}_p = - U$$

With *dop* the doping level, φ the electrostatic potential, ϵ the dielectric constant, *n* and *p* the electron and hole free carrier densities, expressed within Fermi-Dirac statistics. The drift diffusion currents \overrightarrow{J}_n and \overrightarrow{J}_p are [1] :

$$(2) \quad \overrightarrow{J}_n = - q \cdot n \cdot \mu_n \cdot \overrightarrow{\text{grad}} \varphi_n ; \quad \overrightarrow{J}_p = - q \cdot p \cdot \mu_p \cdot \overrightarrow{\text{grad}} \varphi_p$$

where φ_n and φ_p are the electrochemical potentials. These expressions are valid in both homo- and hetero- structures [1]. The electron and hole mobilities μ_n and μ_p are expressed within a field dependant mobility law, such as [2] :

$$(3) \quad \mu_n = \frac{\mu_{n0}}{1 + \frac{\mu_{n0}}{v_{ns}} \cdot |\vec{\text{grad}} \varphi_n|} \quad ; \quad \mu_p = \frac{\mu_{p0}}{1 + \frac{\mu_{p0}}{v_{ps}} \cdot |\vec{\text{grad}} \varphi_p|}$$

where μ_{n0} and μ_{p0} are the low field mobilities, v_{ns} and v_{ps} are the saturation velocities. The U term can include many recombination or generation mechanisms. The more usual are the Shockley-Hall-Read (SHR) deep level thermal recombination generation, Auger recombination, spontaneous band to band recombination, which only depend on local carrier concentrations. For example, U_{SHR} writes [1] :

$$(4) \quad U_{SHR} = \frac{n \cdot p \left(1 - \exp \left(q \cdot \frac{\varphi_n - \varphi_p}{k \cdot T} \right) \right)}{\tau_p \cdot (n + n_1) + \tau_n \cdot (p + p_1)}$$

where τ_n and τ_p are the extrinsic carriers lifetimes. Other generation mechanisms, such as the impact ionization are field dependant. The impact ionization generations, G_{in} and G_{ip} , due to electrons and holes, are given by :

$$(5) \quad G_{in} = \frac{1}{q} \cdot \alpha_n \cdot |\vec{J}_n| \quad ; \quad G_{ip} = \frac{1}{q} \cdot \alpha_p \cdot |\vec{J}_p|$$

The ionization coefficients α_n and α_p are field dependant and not merely potential dependant : the energy of the carriers is a function of the driving fields $-q \cdot \vec{\text{grad}} \varphi_n$ for the electrons, and $q \cdot \vec{\text{grad}} \varphi_p$ for the holes. Thus, the ionization coefficients are expressed as :

$$(6) \quad \alpha_n = \alpha_{n0} \cdot \exp \left(- \frac{E_n}{|\vec{\text{grad}} \varphi_n|} \right) \quad ; \quad \alpha_p = \alpha_{p0} \cdot \exp \left(- \frac{E_p}{|\vec{\text{grad}} \varphi_p|} \right)$$

Therefore, when describing a field dependant mobility law (3), or an impact ionization model (5), (6), fields and currents must be precisely computed at the nodes, with an appropriate centered formulation.

2 RESOLUTION METHOD

We consider that the potentials $(\varphi, \varphi_n, \varphi_p)$ are the fundamental entities describing the device state. So, this leads to a natural choice of unknowns $(\varphi, \varphi_n, \varphi_p)$ for the set of equations (1), which can be written as :

$$(7) \quad \left\{ \begin{array}{l} \operatorname{div}(\epsilon \cdot \overrightarrow{\operatorname{grad}} \varphi) = q \cdot (n(\varphi, \varphi_n) - p(\varphi, \varphi_p) - dop(\varphi, \varphi_n, \varphi_p)) \\ \operatorname{div}(n(\varphi, \varphi_n) \cdot \mu_n(\varphi_n) \cdot \overrightarrow{\operatorname{grad}} \varphi_n) = -U(\varphi, \varphi_n, \varphi_p) \\ \operatorname{div}(p(\varphi, \varphi_p) \cdot \mu_p(\varphi_p) \cdot \overrightarrow{\operatorname{grad}} \varphi_p) = U(\varphi, \varphi_n, \varphi_p) \end{array} \right.$$

with appropriate boundary conditions. This general formulation has been derived from (1) independantly of the mobility law, of the Recombination-Generation term and of the statistics (Maxwell-Boltzman or Fermi-Dirac) used. So, the equation set (7) is adequate to describe a wide range of semiconductor devices including III-V optoelectronic devices.

The domain of definition Ω of the set of equations (7) is a bounded domain belonging to \mathbb{R}^n , ($n \leq 3$). The boundary of the domain, $\Gamma = \partial\Omega$, is divided into classes, each of them corresponding to a given boundary condition type (ohmic contact, Schottky contact and insulating boundary).

2.1 Discretization scheme

The general form of the equations in (7) is of the type :

$$(8) \quad \operatorname{div} a \cdot \overrightarrow{\operatorname{grad}} f = b .$$

This equation is discretized using the general frame of the so called "Box method" [2]. A finite differences type notation together with a rectangular box $\Omega_{i,j}$ surrounding the node (i,j) is used to survey the method (figure 1). After discretization over the box $\Omega_{i,j}$, equation (8) writes :

$$(9) \quad \sum_{k=1}^m \left(\int_{\gamma_k} a_{i,j} \cdot \overrightarrow{\operatorname{grad}} f \cdot \vec{n}_k \cdot d\gamma \right) = \iint_{\Omega_{i,j}} b_{i,j}(f) \cdot d\Omega$$

where m is the number of boundary elements, \vec{n}_k is the unitary vector normal to the boundary element γ_k .

The two fundamental basic hypotheses of the discretization scheme are :

- the scalars $a_{i,j}$ and $b_{i,j}$ are constant inside the box $\Omega_{i,j}$.
- the continuity of the normal component $a \cdot \overrightarrow{\operatorname{grad}} f \cdot \vec{n}$ of the flux density vector is imposed at each boundary of box $\Omega_{i,j}$.

In the case of a rectangular mesh, the box is divided into eight rectangular triangles, so that the f potentials plane by triangular subdomain satisfy the above mentioned hypotheses (figure 1). The quantities with subscripts $(i+\frac{1}{2}, j)$, $(i-\frac{1}{2}, j)$, $(i, j+\frac{1}{2})$ and $(i, j-\frac{1}{2})$ are deduced from the nodal values according to the interpolation formulae derived from the discretization hypotheses. For example :

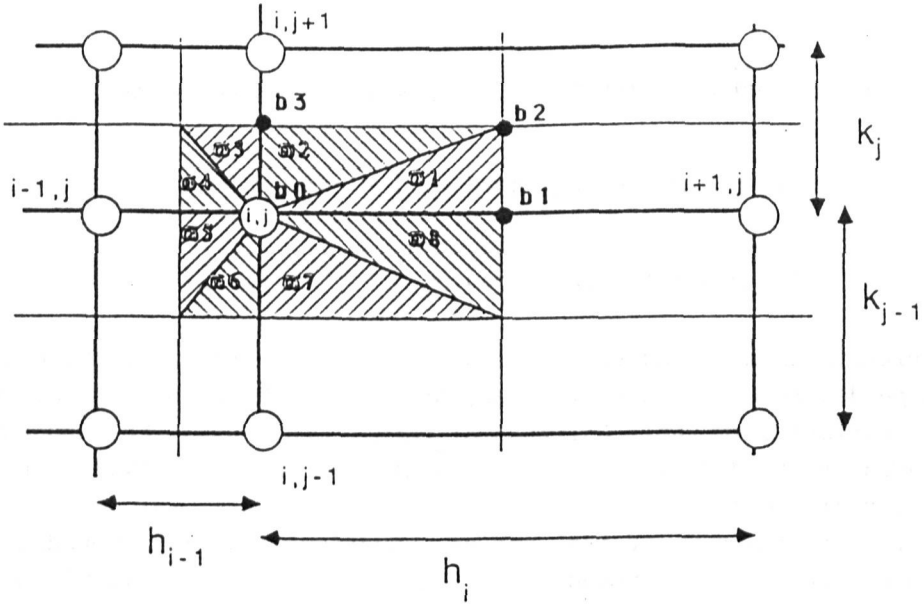


Figure 1 : a rectangular box divided into 8 triangles used in the discretization scheme

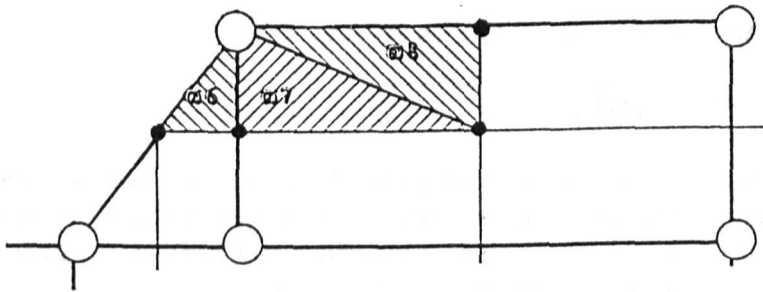


Figure 2 : configuration of a box arising for the description of boundary conditions

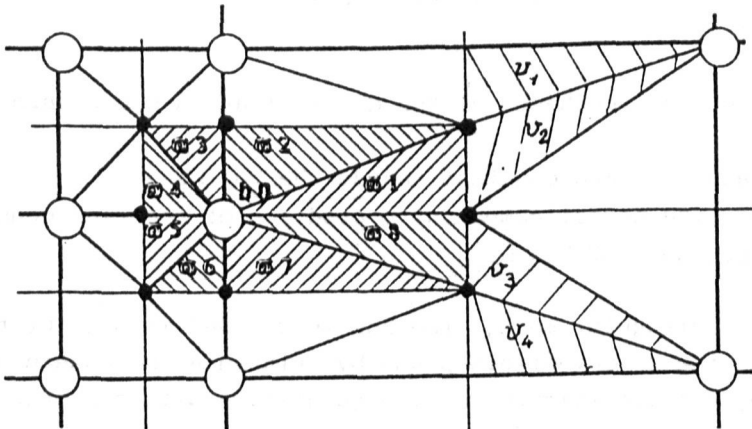


Figure 3 : configuration of a box arising at a terminating line

$$(10) \quad \overrightarrow{a \cdot \text{grad}} f \Big|_{i+\frac{1}{2},j} \cdot \vec{n}_{i+\frac{1}{2},j} = 2 \cdot \frac{a_{i,j} \cdot a_{i+1,j}}{(a_{i,j} + a_{i+1,j})} \cdot \frac{f_{i+1,j} - f_{i,j}}{h_i}$$

Field dependant mobility laws and impact ionization need the computation of the quantities $|\overrightarrow{\text{grad}} \varphi_n|$ and $|\overrightarrow{\text{grad}} \varphi_p|$, as well as the currents densities, at the nodes. These expressions, at the nodes, are obtained by interpolation, using the discretization scheme. Owing to (10), the field of the potentials f , in the x and y directions, can similarly be expressed :

$$(11) \quad \text{grad}_x f_{i,j} = \frac{\left(a_{i-\frac{1}{2},j} \cdot \left(\frac{f_{i,j} - f_{i-1,j}}{h_{i-1}} \right) \cdot h_i + a_{i+\frac{1}{2},j} \cdot \left(\frac{f_{i+1,j} - f_{i,j}}{h_i} \right) \cdot h_{i-1} \right)}{(a_{i-1,j} \cdot h_i + a_{i+1,j} \cdot h_{i-1})}$$

$$(12) \quad \text{grad}_y f_{i,j} = \frac{\left(a_{i,j-\frac{1}{2}} \cdot \left(\frac{f_{i,j} - f_{i,j-1}}{k_{j-1}} \right) \cdot k_j + a_{i,j+\frac{1}{2}} \cdot \left(\frac{f_{i,j+1} - f_{i,j}}{k_j} \right) \cdot k_{j-1} \right)}{(a_{i,j-1} \cdot k_j + a_{i,j+1} \cdot k_{j-1})}$$

The general case uses a "finite boxes" type mesh [3] allowing geometrical description facilities (figure 2) and local refinement (figure 3).

2.2 Resolution

The numerical resolution is classical. After discretization, the equation set is linearized and solved using a Newton-like method [4] :

$$(13) \quad [A] \cdot \delta f = B$$

where δf is the correction vector of the solution (φ , φ_n , φ_p).

Using this discretization scheme, the method is particularly robust even for very poorly adapted mesh. This robustness, due to the interpolation formulae used in (10), allows to obtain an approximated solution in order to refine the initial coarse mesh, until the final mesh-solution satisfies a prerequired precision.

3 AUTOADAPTATIVE MESH REFINEMENT

The refinement is performed by an autoadaptative method. One of the most important point, when dealing with such a method, is to be able to exhibit and evaluate a mesh refinement criterion [5]. The refinement criterion we have developed is computed using an estimation of an error arising from the discretization scheme. Physically, in equation (8), the terms a and b are functions of f . In semiconductor, continuity equations, the discretization error is rather due to the a and b large spatial variations, than to the usual Laplace discretization error. The error computation is local. It uses an a posteriori estimation of the distance $\delta f_{i,j}$ between the computed solution $f_{i,j}$ and the

unknown physical solution, within the box $\Omega_{i,j}$.

3.1 Refinement criterion computation

Let us consider the b term. The discretization scheme is built on the hypothesis that $b_{i,j}$ is constant over the box $\Omega_{i,j}$. The error committed with this hypothesis is evaluated. For this, the physical spatial variations of b are linearized leading to eight plane functions in the box $\Omega_{i,j}$. In the patterned triangle ω_t (figure 1), linearization leads to :

$$(14) \quad b_{\omega_t}(x,y) = b_{i,j} + \left. \frac{\partial b}{\partial x} \right|_{\omega_t} \cdot (x - x_i) + \left. \frac{\partial b}{\partial y} \right|_{\omega_t} \cdot (y - y_j)$$

Taking into account the contributions of each of the eight triangles ω_t , we build $\delta b_{i,j}$, the error on the evaluation of the right member of (9) :

$$(15) \quad \delta b_{i,j} = \sum_{t=1}^8 \left\{ \iint_{\omega_t} \left(\left. \frac{\partial b}{\partial x} \right|_{\omega_t} \cdot (x - x_i) + \left. \frac{\partial b}{\partial y} \right|_{\omega_t} \cdot (y - y_j) \right) dx dy \right\}$$

Owing to (13), the error $\delta f_{i,j}^b$, contribution of b to the error $\delta f_{i,j}$ is :

$$(16) \quad (A_{i-\frac{1}{2},j} + A_{i+\frac{1}{2},j} + A_{i,j+\frac{1}{2}} + A_{i,j-\frac{1}{2}}) \cdot \delta f_{i,j}^b = \delta b_{i,j}$$

In order to compute $\delta f_{i,j}^b$, the method takes full advantage of the geometrical properties of the rectangular bidimensionnal mesh : the function $b(f)$ can be computed at the neighbouring nodes of (i,j) , since f has been computed at these nodes. $\delta b_{i,j}$ needs to be computed and thus also the derivatives of b . For example, in triangle 1 (fig. 1) :

$$(17) \quad \left. \frac{\partial b}{\partial x} \right|_{\omega_1} = 2 \cdot \frac{b_1 - b_0}{h_i} \quad \text{and} \quad \left. \frac{\partial b}{\partial y} \right|_{\omega_1} = 2 \cdot \frac{b_2 - b_1}{k_j}$$

where : (18) $b_1 = b_{i,j}(f_{i+\frac{1}{2},j})$ and (19) $b_2 = b_{i,j}(f_{i+\frac{1}{2},j+\frac{1}{2}})$

Finally with the projections of $\delta b_{i,j}$ over the two coordinate axes, four contributions to the error $\delta f_{i,j}^b$ are derived and expressed at the four boundary points of the box $\Omega_{i,j}$:

$$(20) \quad \left\{ \begin{array}{ll} \delta f_{i+\frac{1}{2},j}^b = \frac{\delta b_{i,j}^x}{A_{i+\frac{1}{2},j}} & ; \quad \delta f_{i-\frac{1}{2},j}^b = \frac{\delta b_{i,j}^x}{A_{i-\frac{1}{2},j}} \\ \delta f_{i,j+\frac{1}{2}}^b = \frac{\delta b_{i,j}^y}{A_{i,j+\frac{1}{2}}} & ; \quad \delta f_{i,j-\frac{1}{2}}^b = \frac{\delta b_{i,j}^y}{A_{i,j-\frac{1}{2}}} \end{array} \right.$$

Similar errors are obtained for the a term in (9).

3.2 Mesh refinement strategy

At two dimensions, the projections (20) over the coordinate axis permit to indicate in which direction the error contribution is the largest. In a given direction, the refinement strategy lies on the symmetrization of the mesh step. In one direction, the first order spatial discretization errors of the terms a and b are null, when the node is at the center of the box, and the computed error is the second order error. The simplified refinement algorithm is :

- Compute the error $\delta f_{i,j}$ in the box $\Omega_{i,j}$.
- IF $|\delta f_{i,j}| \leq \frac{k \cdot T}{q}$ then prerequired mesh-solution precision is reached.
- ELSE
 - IF $\Omega_{i,j}$ is non-symmetrical in the direction of the largest error then
 - refine so $\Omega_{i,j}$ becomes symmetric in the concerned direction.
 - ELSE
 - $\delta f_{i,j}$ is the second order error then
 - refine in the direction of the largest error.
- END IF
- END IF

The action of **refine** consists in dividing by two the concerned step. This strategy allows to implement an efficient autoadaptative anisotropic mesh refinement method.

4 APPLICATIONS

The bidimensional simulator has been used for a scholastic Si p - n junction. The mesh and the electrostatic potential are reported (figure 4) after a few refinement cycles at thermodynamical equilibrium. The initial coarse mesh had 6×6 nodes uniform distribution. The refinement has occurred in both directions, in relation to the curvature of the electrostatic potential. This "Finite Boxes" mesh [3] allows an efficient local refinement method.

The second example deals with a 1D GaAs Field Effect transistor short channel under 5V bias. Figure 5 shows that refinement has occurred according to the negative and positive peaks of fields and velocities, particularly, as it could have been expected, in the saturation region.

The behaviour of heterostructures encountered in III-V optoelectronic devices is far less predictable. Figure 6 shows the band structure of a GaInAs/InP isotype n - n heterojunction under 2V bias. These heterojunction are encountered in many of the optoelectronic devices such as APD or Laser diodes... The location of the nodes of the refined mesh is shown. The initial mesh had only three nodes. Such an autoadaptative mesh generator is essential to describe such unpredictable mesh for III-V devices made of heterojunctions [6].

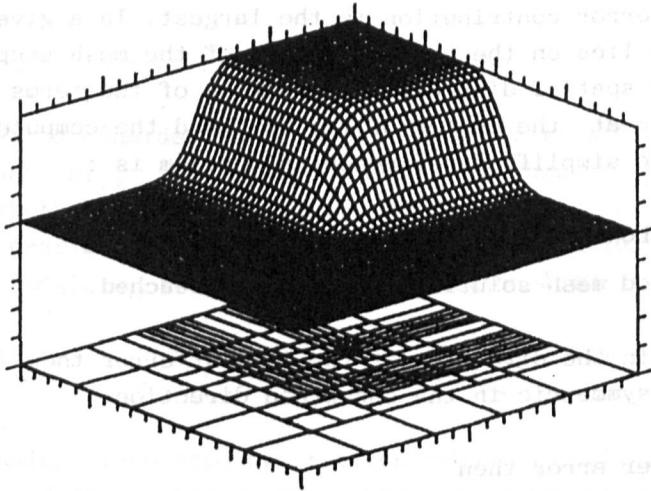


Figure 4 : electrostatic potential map over the refined mesh. (Si p-n junction)

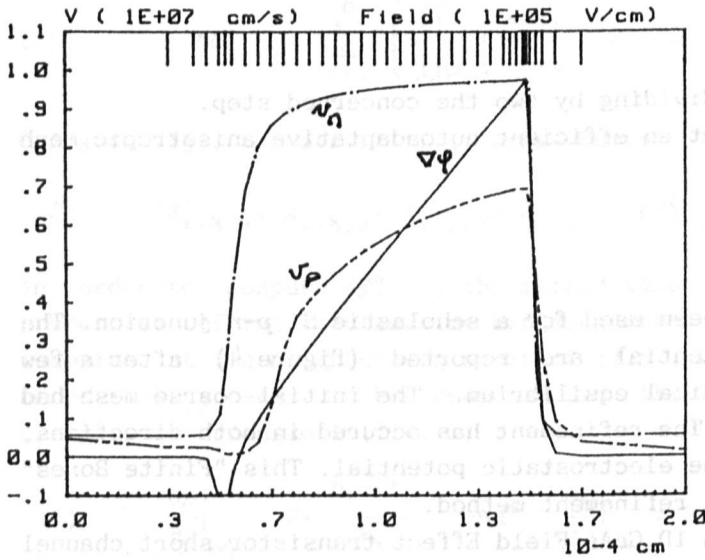


Figure 5 : field and velocities with the locations of the nodes after mesh refinement. (GaAs FET channel, 5 Volts bias)

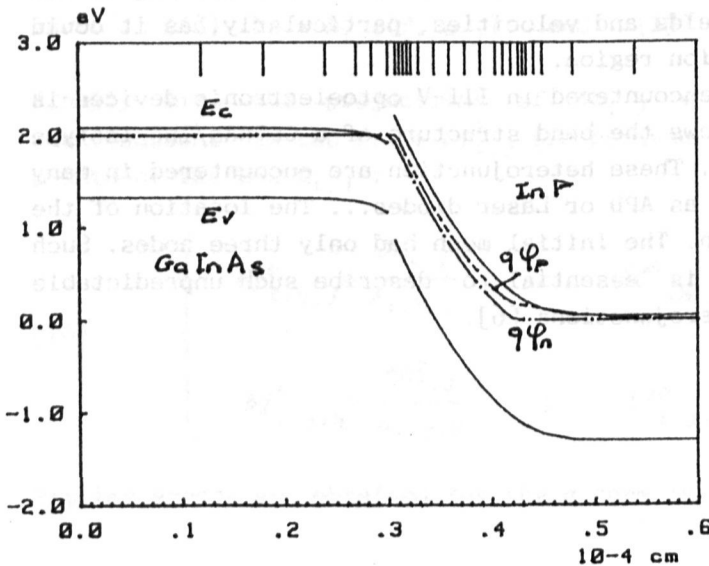


Figure 6 : band structure and locations of the nodes after mesh refinement. (GaInAs/InP n-n heterojunction under 2 Volts bias)

5 CONCLUSION

In the semiconductor devices simulation physical model, we stress on two different features : the equations have a common form and include fields and current at the nodes. We then show how a discretization scheme deals with these two features. This scheme allows the computation of the associated error, criteria of a refinement method and to its autoadaptive implementation. It also yields great robustness to the solving method. Refinement and robustness permit the simulation of the devices we were first concerned with.

REFERENCES

- [1] J.E. Viallet and S. Mottet, "Heterojunction under Fermi-Dirac statistics: general set of equations and steady state numerical methods", Proceedings of NASECODE IX Conf., Boole Press, pp. 530, (1985).
- [2] S. Selberherr, "Analysis and Simulation of Semiconductor Devices", Springer Verlag, Wien, New-York (1983)
- [3] A.F. Franz and all "Finite Boxes - A generalisation of the finite difference method suitable for semiconductor device simulation", IEEE Trans. ED, Vol. ED 30, No 9, pp. 1070-1082, (1983)
- [4] R. Bank, D.J. Rose and W. Fichtner, "Numerical methods for semiconductor device simulations", IEEE Trans Electron devices, Vol. ED-30, No 9, pp. 1031-1041, (1983).
- [5] P. Ciampolini and al, "Adaptive mesh generation preserving the quality of the initial grid", IEEE Trans CAD of ICAS, Vol CAD-8, No 5, pp. 490-500, (1989).
- [6] S. Mottet and J.E Viallet, "Electrical 2D simulation of 1.3 μm semiconductor lasers", SISDEP Vol 3, pp. 637-648, (1988).